An experimental investigation of the combined influence of notch size and fibre orientation on the fatigue strength of a short glass fibre reinforced polyamide 6

Andrea Bernasconi [a, *], Edoardo Conrado [a], Peter Hine [b]

[a] Dipartimento di Meccanica, Politecnico di Milano, via La Masa 1, 20156 Milano, Italy
[b] Soft Matter Physics Research Group, School of Physics and Astronomy, University of Leeds, Leeds LS2 9JT, UK

Received 1 July 2015
Accepted 5 August 2015
Available online 10 August 2015

1. Introduction

Interest in the fatigue behaviour of Short Fibre Reinforced Polymers (SFRP) is growing steadily because these materials offer opportunities of cost and weight saving in many industrial sectors, such as automotive, furniture and home appliances. SFRPs are employed for manufacturing mass production components, which may undergo significant mechanical cyclic loading, in the framework of metal replacement. However, the use of SFRPs calls for fatigue strength assessment methods different from those usually employed for metals.

This is mainly due to the intrinsic anisotropic nature of SFRPs and to the peculiar mechanical behaviour of the thermoplastic polymeric matrix, which is often prone to temperature, frequency and humidity effects. The latter effects on fatigue behaviour of SFRPs have been studied and results reported in a large number of publications. Here we mention only some concerning polyamides [1–7], which is the material investigated in this work, often performed using standard dumbbell specimens. The effects of anisotropy are strictly related to the fibre orientation distribution in the final component, which in turn depends on the manufacturing route, which is usually injection moulding. This widely employed manufacturing method can set up complicated velocity fields in the mould during manufacture, leading to inhomogeneous fibre structures which may differ from the fibre structure found in standard specimens.

Thus, the assessment of orientation effect was often performed by off axis tests, using specimens cut from injection moulded plates [8,9]. This allows for assessing the effect of fibre orientation in the presence of a relatively uniform fibre structure and, consequently, a relatively uniform stress distribution. However, in real parts, their often complex geometry usually determines fibre orientation patterns which differ from those encountered in standard specimens or in specimens extracted from plates. Moreover, stress concentrations arise due to the presence of notches (e.g. at locations where stiffening ribs meet each other) [10]. Consequently, this calls for conducting tests on notched specimens to evaluate the notch effect. This constitutes a necessary intermediate step towards the defini-tion or the validation of any procedure for the fatigue assessment of real parts.

The notch effect on the fatigue strength of short glass fibre reinforced polyamides had been studied by means of

* Corresponding author.
E-mail address: andrea.bernasconi@polimi.it (A. Bernasconi).

experimental tests conducted on notched specimens [11–13]. In Ref. [11], it was shown that the fatigue strength decreases with increasing hole diameter, but not with relative hole diameter (i.e. diameter divided by the net gauge section), although a reduction with respect to the unnotched specimen was still observed. It is worth noting that holes were drilled, not obtained by moulding. In Ref. [12,13], specimens with mild and sharp notches were manufactured by injection moulding and tested in the dry as-moulded state. Under these conditions, a strong sensitivity to notches was found. In the aforementioned works, no description of the fibre orientation pattern at the locations where failure initiated was reported. Moreover, the role of crack propagation was not investigated.

In order to transfer results of tests on specimens to real parts for fatigue assessment purposes, knowledge of the fibre orienta-tion in the specimens is of fundamental importance. Such mea-surements can help to decouple the effects of geometry (for instance notch radius) and local fibre orientation structures caused by that local geometry. Although modelling is not addressed in this paper, we believe that this information could be useful in subsequent analyses, e.g. based on local stress distri-butions, like in Ref. [14].

In the present study, the results of an experimental investigation on the combined effect of notches and fibre orientation on the fatigue strength of a polyamide 6 reinforced with short glass fibre are presented and analysed. The present research follows the path traced by a previous work [15] where the effect of circular notches having a relatively large radius of 7.5 mm was studied for small injection-moulded plates, in conjunction with the effect of different fibre orientation patterns obtained by varying the type and position of the injection gate.

In the present work, the combined effect of fibre orientation and notches with dimensions close to the ones of real applica-tions was investigated. The mould employed in Ref. [15] was modified in order to obtain small plates with lateral V-shaped notches with tip radii of 0.5, 1 and 2 mm. All three types of specimen were injection moulded through either a film gate on the top face of specimens or a side gate on a lateral face of the specimens. In this way, the combined effect of notches and fibre orientation distributions was studied for different values of the notch tip radius. Then, the fibre orientation distribution was analysed experimentally, and its relationship with the observed fatigue behaviour investigated, also considering the fatigue crack propagation phase.

2. Experimental

2.1. Mechanical testing

Static and fatigue tests were performed on specimens made of injection-moulded polyamide 6 reinforced with 30% by weight of short E-glass fibre (PA6 GF30). For this material, the nominal fibre diameter was 10.5 μm and the number and weight average fibre length was 220 μm and 275 μm, respectively (values measured after the injection-moulding process). The specimen shape and dimensions are shown in Fig. 1. The specimens consisted of small plates, 150 mm long, 45 mm wide and 3.2 mm thick, characterized by the presence of two lateral V-shaped notches symmetrical with respect to the longitudinal mid-section of the specimen. They were obtained by means of an injection moulding process in which the design of the mould allowed for the use of two different feed system layouts, as in Ref. [15]. In one layout, the specimen was injected through a film gate located on the top face of the specimen in order

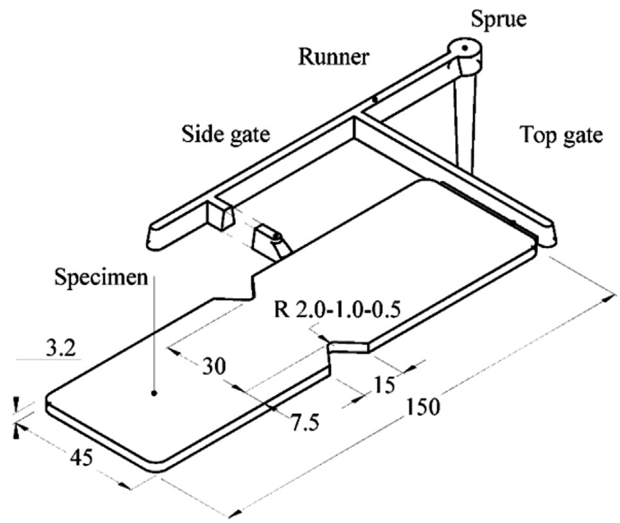

Fig. 1. Shape and dimensions of the specimen and layouts of the feed system.

to induce a longitudinal melt flow during cavity filling. The use of this feed system, as reported in Ref. [15] and successively confirmed in Ref. [16], resulted in a symmetric fibre orientation distribution that was predominantly longitudinal. In the other one, a side gate located on a lateral face of the specimen induced asymmetric filling of the specimen cavity, causing a less homogeneous fibre orientation distribution.

For the manufacture of the specimens studied in this work, the mould was equipped with interchangeable inserts so that three different notch tip radii could be obtained, namely 0.5, 1 and 2 mm, with the same net cross-section width equal to 30 mm. A total of six test specimen batches were manufactured and used for tensile and fatigue tests, comprising all combinations of the three different notch tip radii and longitudinal or lateral injection. The material was conditioned prior to testing in order to obtain a matrix in hygro-thermal equilibrium with an ambient temperature of 23 °C and a relative humidity of 50%.

Uniaxial static and fatigue tests were performed at Politecnico di Milano using an Instron 8501 servo-hydraulic dynamic test system with a load capacity of 100 kN. All the tests were conducted at a controlled room temperature of 23 °C (±2 °C) in an air conditioned laboratory environment with uncontrolled humidity. The quasi-static tensile tests were carried out at a crosshead speed of 5 mm/min. The fatigue tests were performed in the range of cycles to failure from 10^3 to 10^6. These tests were load controlled tension–tension fatigue tests in which sinusoidal load cycles with a load ratio R = 0.1 (i.e. the ratio of minimum to maximum applied load) were applied at a constant frequency.

The load frequency was set to 4 Hz as a compromise between available test time and limitation of specimen self-heating. In Ref. [12] it was reported that, for notched specimens, high frequency is allowed because, for this type of specimen, the maximum stressed volume is much smaller than the specimen's volume, and the heat generated in the maximum stressed volume can be dissipated to the next less stressed and less warm volume of material. However, local temperatures were not measured during our tests. The failure criterion for fatigue tests was specimen separation. In these tests, if the failure criterion was not met by 10^6 load cycles, the tests were interrupted (run-out).

2.2. Fibre orientation analysis

In order to investigate any possible correlations between the fatigue behaviour and the fibre orientation distributions at notches induced by the different injection gate types and positions, experimental analysis of specimen microstructure was carried out. Measurements of fibre orientation distributions were performed by means of the optical section method. In this method, 2D polished sections were taken from the area of interest and then evaluated using an in-house image analysis facility developed at the University of Leeds [17]. Each fibre that meets the 2D section is seen as an elliptical footprint, and measuring the ellipticity and the orientation of the major axis of these images allows the two polar angles θ and ϕ that specify the orientation of each fibre (with respect to the reference frame shown in Fig. 2) to be determined.

Results can be presented in various ways, and Fig. 3 shows two examples for a section taken between the sample notches in the YZ plane. First, the results can be displayed as a spatial grey scale map of the average value of a chosen second order tensor average (for instance $<\cos^2 \theta_X>$, as shown in Fig. 3). This representation is useful for identifying the inner fibre structure, such as the centrally located core region (preferred Y axis orientation) shown here. For this visualization, a white pixel indicates a high level of orientation with respect to the X axis (which here is the flow direction) in that region. A more quantitative representation can be achieved by plotting average values of the three second order tensor averages over the scanned area. As the interest in this papers concerns the orientation at the notch root, results are presented as average values across the sample thickness (as shown by the rectangle on the top of Fig. 3). Average values through the thickness are then plotted as a function of the distance across the sample width (between the notches along the Y axis), in order to visualize and compare results.

2.3. Fatigue crack propagation

In order to identify cracks and monitor their propagation, a travelling microscope was used with a back light configuration, as shown in Fig. 4. By exploiting the partial transparency of the polyamide matrix, it was possible to highlight fatigue damage and locate it with respect to the notch tip on the specimen face, but not through the specimen thickness. The fatigue damage appeared in the form of black areas (not present in the undamaged state, see Fig. 5(a)), presumably due to the variation of transparency caused by plastic deformations and initial fibre-matrix debonding (Fig. 5(b)), which eventually formed a crack as the number of cycles increased, as shown in Fig. 5(c). Tests were conducted on specimens injected laterally, since in these specimens a single crack formed at one notch root, while it was observed that in specimens injected longitudinally cracks appeared almost simultaneously at both notches.

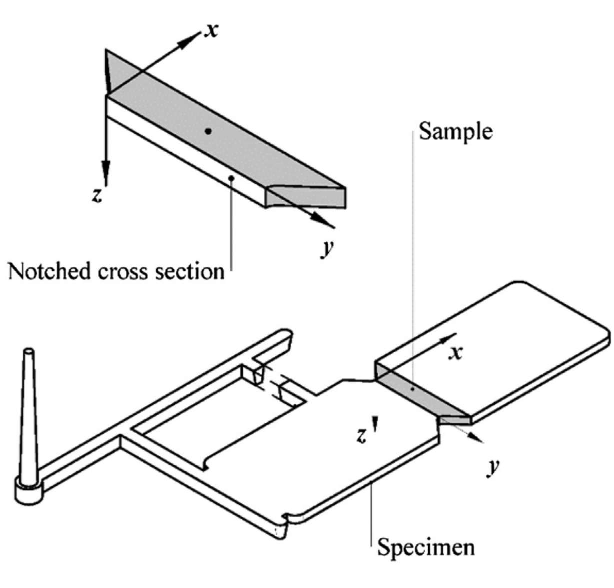

Fig. 2. Visualization of the sample cut out from the test specimen for fibre orientation measurements along with the reference system adopted.

3. Results and discussion

3.1. Results of static tests

Prior to performing fatigue tests, three tensile tests were conducted for each type of specimen, i.e. for each combination of the three notch tip radii and the two different feed system layouts. The results of some of these tests, one for each specimen type, are shown in Fig. 6. In these diagrams, the nominal stress, i.e. the ratio of applied load to initial net cross-section area of the specimen, is plotted against the displacement of the crosshead of the testing machine. The values of the ultimate tensile strength (UTS), i.e. the maximum nominal stress, averaged over the three quasi-static tensile tests conducted for each specimen type, are listed in Table 1. We also report the values obtained in Ref. [15] for the case of a 7.5 mm notch radius and those obtained in Ref. [8] for the case of unnotched specimens, i.e. standard ISO 527-2 Type 1A specimens, made of the same material, even though not belonging to the same batch.

It can be noted that, for the same layout of the feed system, the difference in the static strength for the specimens having a notch tip radius equal to 1, 2 and 7.5 mm was negligible, while in the case of a notch tip radius equal to 0.5 mm a reduction of 5% was obtained respect to the previous cases. Considering specimens with the same notch tip radius, the variation of the injection location from the top to the side resulted in a reduction of about 15% in terms of the maximum load reached during the tests for all the three values of the notch tip radius.

3.2. Results of fatigue tests

Fatigue tests were carried out at different load levels in order to characterize the fatigue strength of the PA6 GF30 in the presence of V-notches with various notch root radii in a range from 10^3 to 10^6 load cycles. The results of the fatigue tests performed on specimens injected in the longitudinal direction are shown in Fig. 7(a), while those obtained from specimens laterally injected are shown in Fig. 7(b). The fatigue test results are reported in diagrams on log–log scales in which the maximum applied nominal fatigue stress σ_{max}, i.e. the ratio of maximum applied load to the initial net area of the specimen cross-section, is plotted against the cycles to failure N_f. In order to obtain nominal stress–life curves, the experimental data were interpolated using a Basquin relation, that is:

$$\sigma_{max} = \sigma'_f N_f^{-b}$$

The values of the material parameters of this equation, the fatigue strength exponent b and the fatigue strength coefficient σ'_f, were determined by means of linear regression on experimental data, and are listed in Table 2. The obtained stress–life curves, actually straight lines in a log–log diagram, are plotted for each batch of specimens, in Fig. 7.

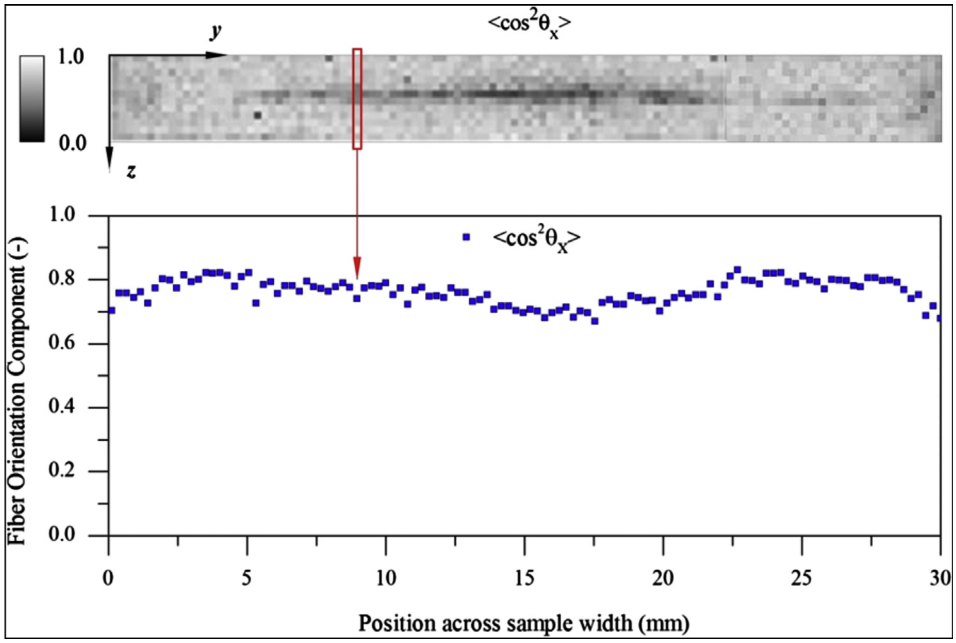

Fig. 3. Visualization of fibre orientation analysis results.

3.3. Analysis of fibre orientation

3.3.1. Influence of gate size and position

The fibre orientation distribution was analysed in the gauge section of one specimen for each batch, using the method described in Section 2.2. Results are presented in terms of average values of $< \cos^2\theta_X >$, $< \cos^2\theta_Y >$ and $< \cos^2\theta_Z >$, which is the average of the square of the cosine of the angle between the fibres and the structural axes of the sample, as defined in Fig. 2. Averaging is performed through the thickness of the gauge section of each specimen.

The values of $< \cos^2\theta_X >$, $< \cos^2\theta_Y >$ and $< \cos^2\theta_Z >$ for the samples having notch root radius of 2 mm injected longitudinally and laterally are shown in Fig. 8(a) and Fig. 8(b), respectively. It appears that, by using the side gate, we obtained a different fibre orientation. In the case of injection through the top edge gate, fibre orientation is symmetric and fibres are mainly aligned longitudinally. In the case of injection through the side gate, fibres have a lower degree of alignment along the stresses acting in the gauge section. Moreover, the fibre orientation pattern is not symmetric, thus offering a possible explanation for the observed different global mechanical behaviour (Figs. 6 and 7) between specimens having the same notch root radius, but different injection gates. The average values of $<\cos^2\theta_x>$ across the sample between the notches was 0.76 for the top injection and 0.70 for the side injection. The sample with the top injection had a corresponding higher stiffness and strength as seen in Fig. 6.

The asymmetric fibre distribution is likely to result into asymmetric stress distribution, as shown by means of numerical analyses presented in Ref. [14]. These analyses were based on a Through Process Modelling (TPM) approach to the fatigue strength assessment of SGFRP [18]. By simulating the injection-moulding process, the fibre orientation distribution was predicted numerically. Then, local mechanical properties were evaluated on the basis of the local values of the fibre orientation tensor and, finally, the stress distribution was obtained taking into account the local mechanical properties of the material.

3.3.2. Influence of the notch tip radius

Results displayed in Fig. 7 and Table 2 show that the variation of the notch tip radius from 2 to 1 mm, for both longitudinally and laterally injected specimens, does not influence significantly the fatigue strength, as previously observed also in the case of static strength. On the contrary, when the notch tip radius is further

Fig. 4. The set up for fatigue crack monitoring.

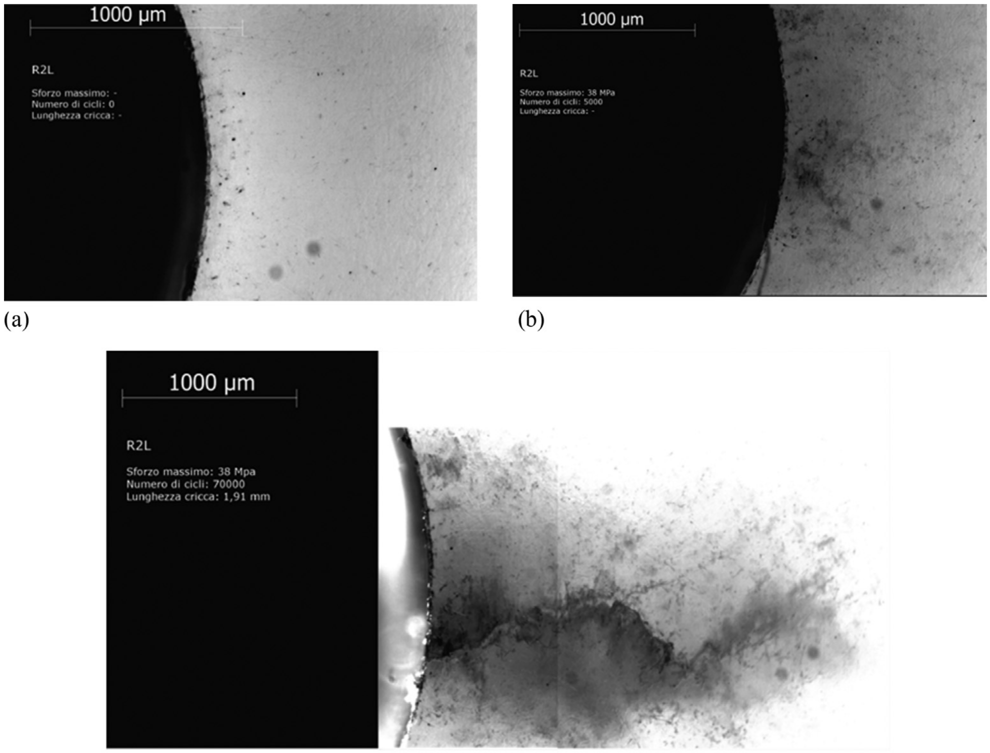

(a) (b) (c)

Fig. 5. Observations of fatigue damage: (a) undamaged state, (b) initial damage and (c) fully developed damage.

reduced to 0.5 mm a non-negligible reduction of the fatigue strength is observed, particularly at high number of cycles, while at low number of cycles this reduction tends to vanish. The fatigue strengths at 1 million load cycles listed in Table 3 confirms and quantifies this observation.

In order to discuss this effect, it is interesting to compare these results with those presented in Ref. [15] and reported in the last rows of Table 2. These tests were carried out on specimen constituted by small plates with two symmetric lateral circular notches with a radius of 7.5 mm and having the same net cross-section area of those of the present study. Although these tests have been conducted with the same test conditions used in the present study, this comparison has some limitations since the tests have been conducted at a frequency of 2 Hz, not at 4 Hz as in the test presented here (moreover the material did not belong to the same batch). Nevertheless, the comparison of the maximum nominal stress at 1 million load cycles, calculated using the material coefficients of the Basquin equation listed in Table 2 and reported in Table 3, shows again that significant differences in the fatigue strength occur only in the case of specimens with a notch tip radius of 0.5 mm.

Fig. 9 shows the results of fibre orientation measurements for samples injected at the top for the three notch tip radii. In gen-eral, the fibres lie in the plane of the plate (XY), although there is a small amount of out of plane orientation (Z axis) at the tip of the notch. The most interesting observation is that the degree of X orientation at each crack tip (and hence the number of fibres that are perpendicular to the crack plane) is lower in the sample with the smaller notch. Similar results were obtained for the case of lateral injection. These observations offer a possible explana-tion for the reduction of strength in the case of the 0.5 mm radius. Previous fracture experiments [19] have shown that the fracture toughness is strongly correlated with the average fibre orientation at the crack tip. In particular, the lower the number of fibres perpendicular to the crack plane (in this case the X axis) the lower the fracture toughness. It is, therefore, proposed that one possible contribution to the lower fatigue strength of the 0.5 mm radius sample is the unfavourable local fibre orientation distribution at the notch tip.

3.4. Role of fatigue crack propagation

Crack nucleation and propagation phases were monitored by means of the optical microscope and the backlighting method described in Section 2.3 using three laterally injected specimens, having the three different values of the notch tip radius of 0.5, 1 and 2 mm and loaded at the same value of the maximum nominal stress ($\sigma_{max} = 38$ MPa and $R = 0.1$). The notch zone was monitored at fixed intervals of number of cycles (from 3000 to 5000 cycles, depending on the expected total life, which in turns depended on notch severity). We looked at the notch opposite the injection gate since it was the one with the highest likelihood of crack nucleation and propagation due to the higher stress concentration on this side of the laterally injected speci-mens, as induced by their asymmetric fibre orientation distribution.

The fatigue damage evolution, i.e. crack nucleation and propagation, was documented by means of magnified images, like those reported in Fig. 5, of the near notch tip zone taken during the tests on specimens with notch tip radii. From these images, it was possible to identify the occurrence of possible plastic deformation and damage initiation, characterized by the appearance of dark areas near the notch tip like that reported in Fig. 5(b). These features appeared at an early stage, namely after 5000 cycles for the

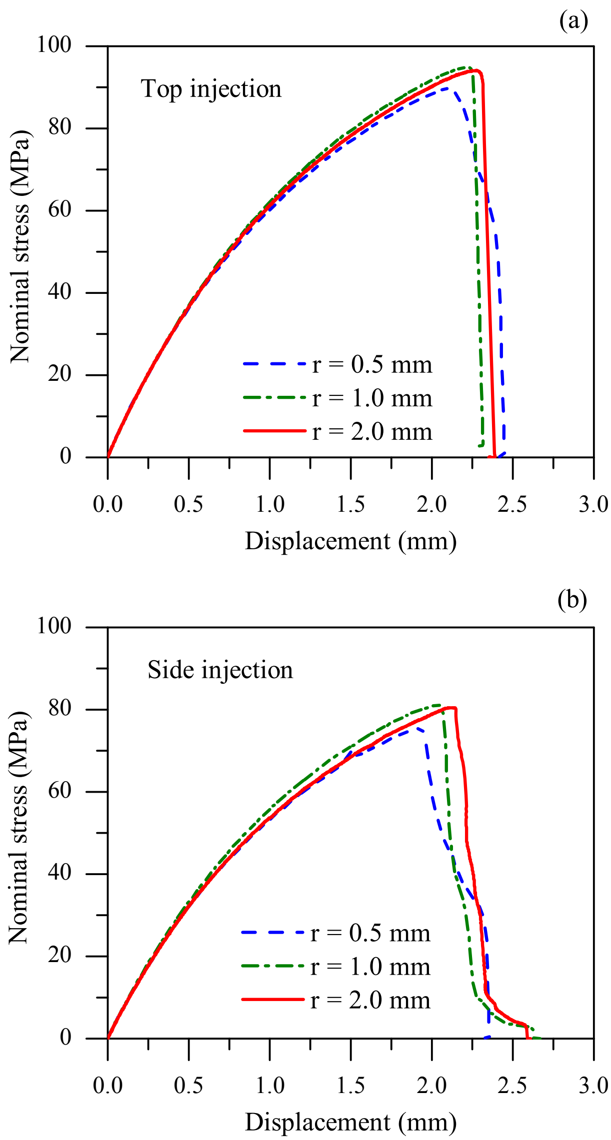

Fig. 6. Comparison of three force–displacement curves obtained by quasi-static tensile tests on specimens with different values of the notch tip radius, r: (a) top injection and (b) side injection.

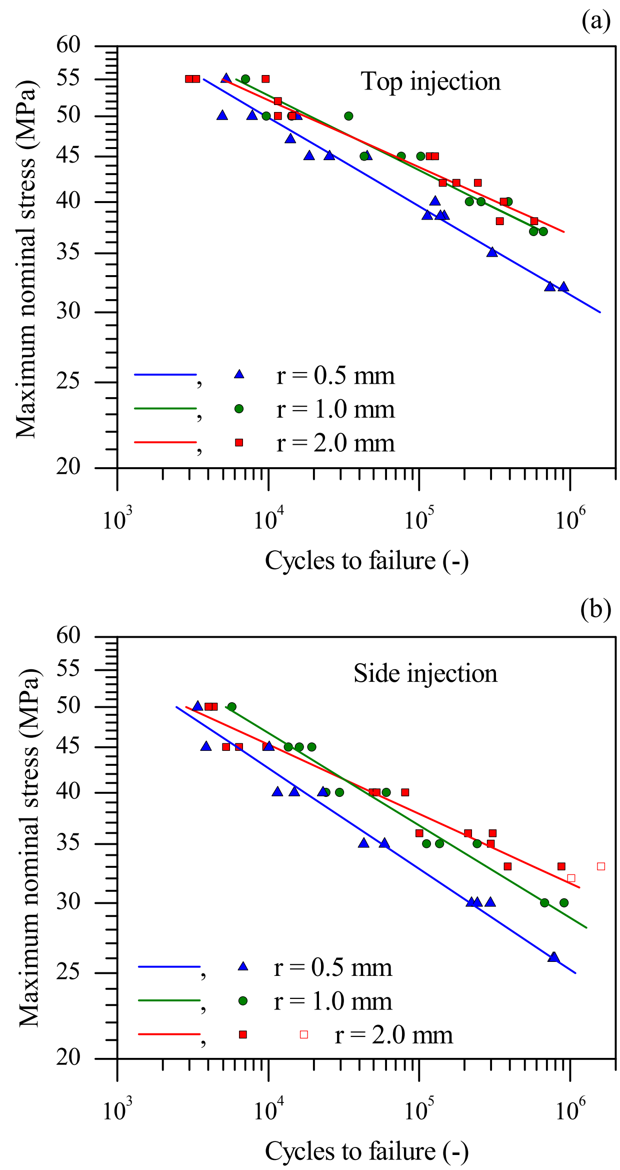

Fig. 7. Results of fatigue tests performed on specimens with different values of the notch tip radius, *r*, (a) injected through a film gate located on the top face; (b) injected through a side gate located on a lateral face.

2 mm notch (Nf = 72,500), 3500 cycles for the 1 mm notch (Nf = 73,500) and 3000 cycles for the 0.5 mm notch (Nf = 19,400). The aspect of these features remained stable for several cycles in the case of 2 mm and 1 mm notch radius, until a detectable crack developed and started propagating after 30,000–35,000 cycles. The propagation in the 0.5 mm specimen started earlier, after only 6000 cycles.

After the nucleation phase, using these magnified images, it was possible to measure crack length during the tests, i.e. monitor crack growth. The results of these measurements are reported in

Table 1
Ultimate tensile strength.

Notch radius	Top gate	Side gate
r (mm)	σ_R (MPa)	σ_R (MPa)
0.5	89.1	75.6
1.0	94.7	80.5
2.0	94.3	79.3
7.5[a]	94	78
Unnotched[b]	104.8	

[a] Results obtained for circular notches reported from Ref. [15].
[b] Results obtained for specimen ISO 527-2 type 1A reported from Ref. [8].

Table 2
Fatigue strength coefficient, σ'_f, and exponent *b* of the Basquin equation.

Notch radius	Top gate		Side gate	
r (mm)	σ'_f (MPa)	*b* (−)	σ'_f (MPa)	*b* (−)
0.5	125.5	0.100	121.8	0.114
1.0	115.1	0.085	122.4	0.105
2.0	105.2	0.076	93.2	0.078
7.5[a]	96.6	0.064	88.1	0.073

[a] Results obtained for circular notches reported from Ref. [15].

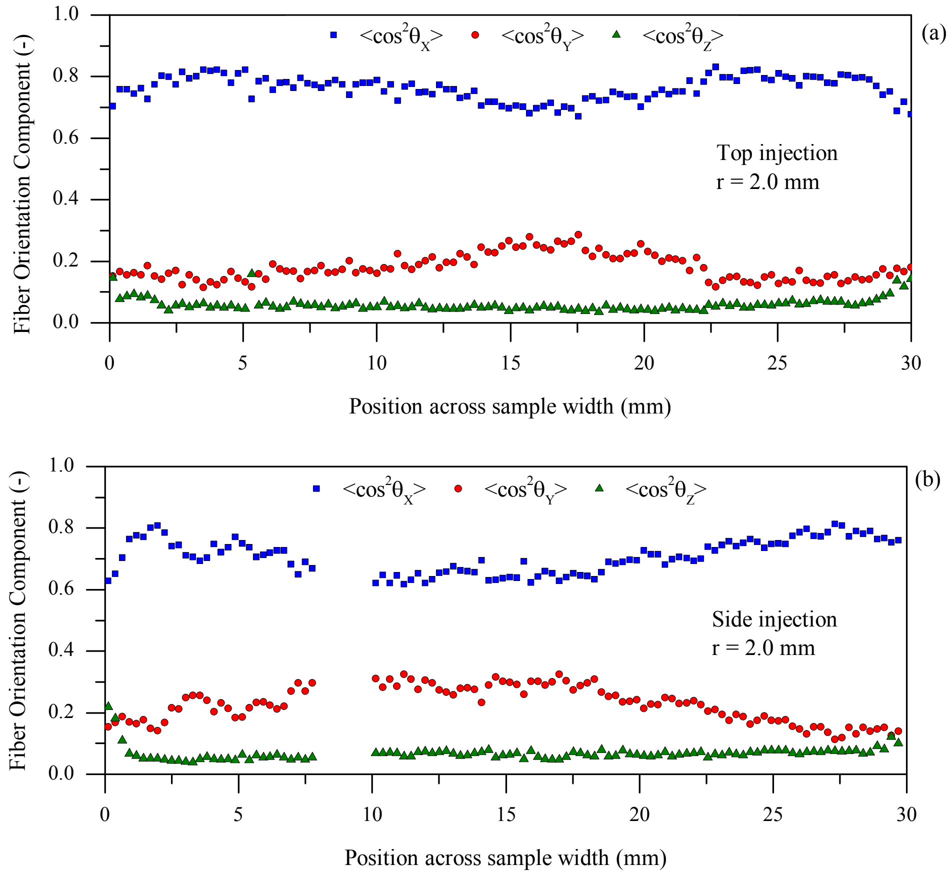

Fig. 8. Results of fibre orientation analysis (YZ section plane) for the specimens with notch root radius of 2 mm: (a) top injection and (b) side injection.

Table 3
Fatigue strength at 1 million load cycles.

Notch radius	Top gate	Side gate
r (mm)	σ_w (MPa)	σ_w (MPa)
0.5	31.4	25.2
1.0	35.7	28.9
2.0	36.7	31.6
7.5[a]	39.9	32.0

[a] Results obtained for circular notches reported from Ref. [15].

the graph of Fig. 10, where the crack length is reported as a function of the percent fatigue life, i.e. the number of cycles at which the crack was observed divided by the number of cycles to failure. This allows for evaluating the percentages of the specimen fatigue life spent in the nucleation and propagation phases as a function of notch radius. At relatively high values of the notch radius, namely 2 and 1 mm, the fatigue life at this stress level was nearly equally subdivided in the nucleation and propagation phases. On the other hand, the smallest value of the notch tip radius, 0.5 mm, resulted in a very short nucleation phase (15% of the total life) and a larger percentage of the total fatigue life spent in the propagation phase. It appears that the crack propagation phase is not negligible in all three cases, with a more pronounced effect in the case of the sharper notch of 0.5 mm radius, which might have been weakened by unfavourable fibre orientation, as shown in Section 3.3.

Concerning crack propagation paths, no significant differences between side injected specimens with different notch tip radii were observed. As shown in Fig. 11, in all the side injected specimens tested, a crack nucleated at the notch opposite to the injection gate and, then, propagated following a slightly curved path turning to-wards the injection gate. In the final rupture phase, the crack changed its path abruptly, becoming nearly straight and transversal to the specimen longitudinal direction. A crack was formed near the notch tip on the side of the injection gate as well, but its nucleation time and propagation speed were always lower than that of the crack on the other side. On the contrary, in specimens injected longitudinally, cracks nucleated and propagated in parallel from both sides, as could be expected due to symmetry of the fibre orientation distribution of these specimens. The propagation fol-lowed a macroscopically straight path, nearly transversal to the specimen longitudinal direction, until the two cracks merged together in the final rupture phase.

The evolution of fatigue damage in notched specimens appeared to be different from that observed in unnotched standard specimens, where diffuse damage is usually observed, whereas in notched specimens damage concentrates at notch root locations and rapidly evolves into crack propagation. However, the fracture surface presented the usual micro-ductile and micro-brittle features, described by Horst et al. [20], corresponding to the crack propagation and final fracture, respectively. The analysis of the fracture surfaces allowed identification of the transition from micro-ductile to micro-brittle in the tested specimens, see Fig. 12. This transition appeared to have taken place well beyond the position of the crack tip at the last recording (e.g. 29 mm from the notch root, while during the last recording, 130 cycle before

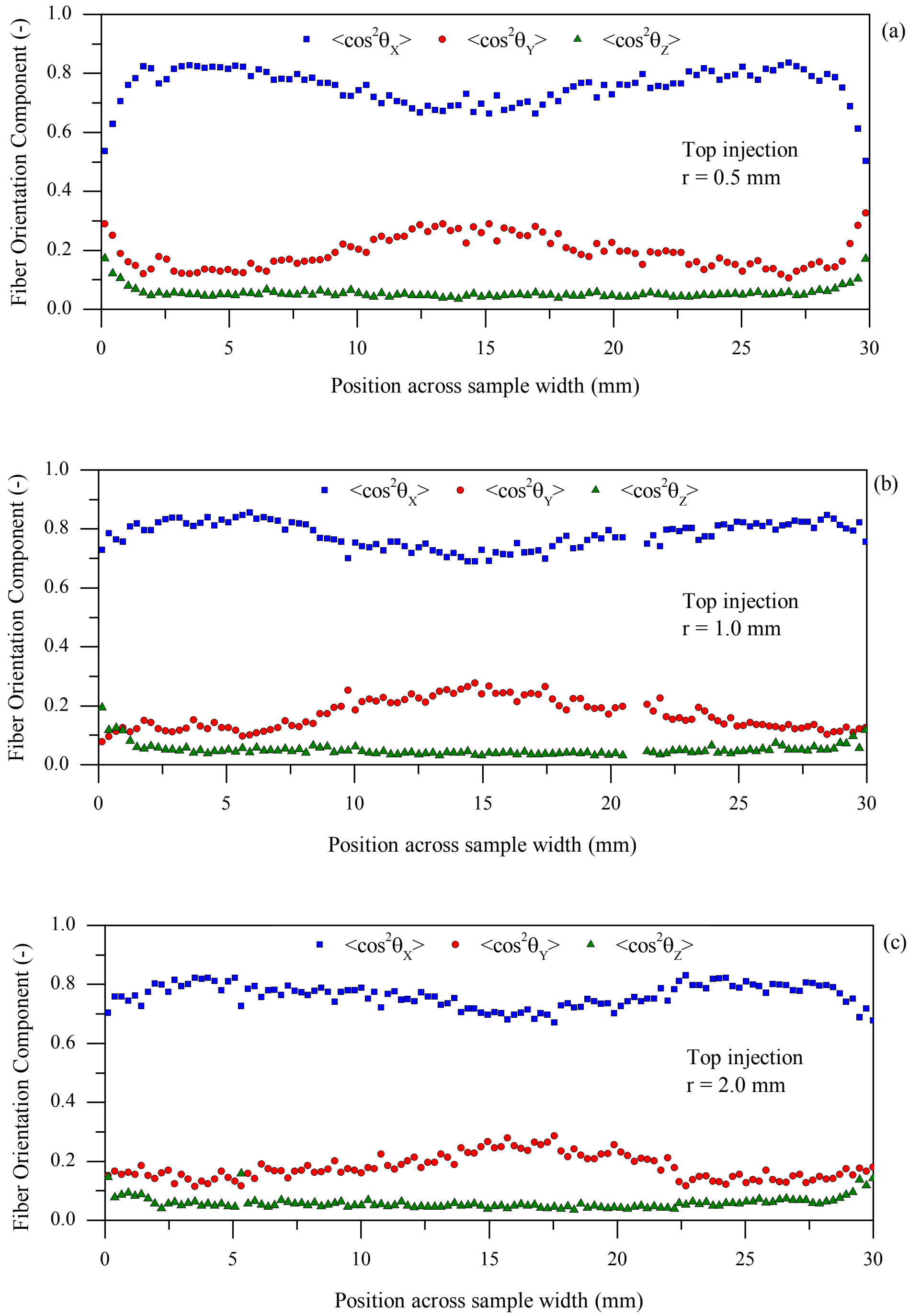

Fig. 9. Results of the fibre orientation analysis for the specimens injected longitudinally (top gate), with different notch root radius values: 0.5 mm (a), 1 mm (b) and 2 mm (c).

fracture, the crack tip position was at 12 mm). However, we believe that this difference was due to fast crack propagation during the last cycles, from the last observation of the crack tip position to final failure. In order to prove this, we interrupted one test before failure and fractured the specimen cryogenically. In this case, the position of the crack tip and the transition were almost coincident, as shown in Fig. 13.

3.5. Role of temperature

As mentioned in Section 2, no field measurement of the surface temperature was conducted, e.g. using thermographic techniques [21]. Therefore, it was not possible to quantify the effect of notch severity on self heating, as in Ref. [22]. Possible higher local temperatures reached in the 0.5 mm notch case might have contributed to lower the fatigue strength and, at the same time, similar local heat buildup could have explained the invariance of fatigue strength with notches of radius in the range from 1 mm to 7.5 mm.

Nevertheless, preliminary analyses [14] showed that by taking into account only the fibre orientation distribution and the corresponding local mechanical properties in finite element models, the

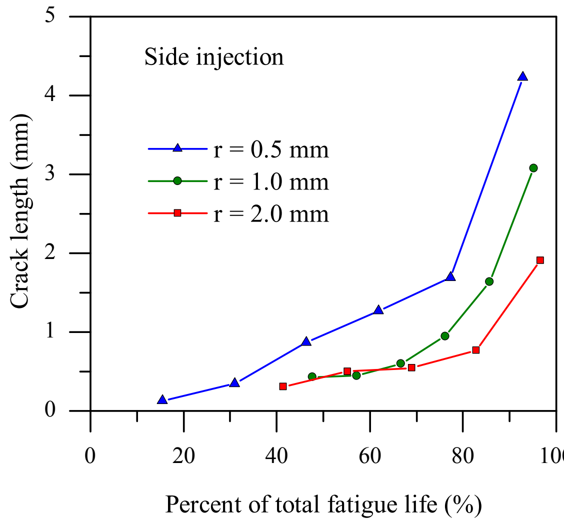

Fig. 10. Measured crack length as a function of the percent of total fatigue life.

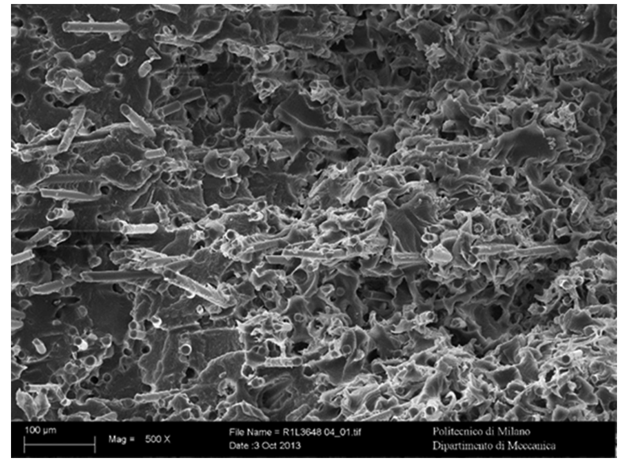

Fig. 12. Transition from the micro-ductile and the micro-brittle area.

observed differences in the fatigue behaviour with different injection gates were explained for notch radii of 2 mm. Therefore, we believe that the whole data set presented herein could be used for further numerical analyses, aimed at assessing the capabilities of the TPM approach.

4. Conclusions

The experimental investigations conducted on injection moulded, notched specimens made of short fibre reinforced polyamide allowed assessing experimentally the combined influence of the fibre orientation and notch root radius on fatigue strength.

In particular, top and side injections of the specimens resulted in different strengths, both in quasi-static and fatigue tests. The measurements of fibre orientation in the gauge section of the specimens showed that the lower strength of side injected specimens can be related to their asymmetric distribution of fibre orientation and to the lower mean value of the degree of fibre alignment in the longitudinal direction.

A small influence of the notch tip radius on the static and fatigue strength of notched specimens was found for both top and side injected specimens, and for all the values of the notch tip radius except for the minimum value investigated, r = 0.5 mm. In this latter case, the optical measurements of fibre orientation showed, in the near notch root area, a significant drop of fibre alignment in the longitudinal direction, giving a possible explanation for the significant strength reduction experimentally observed, and pointing out the importance of fibre orientation analysis at critical areas such as the root of the notch.

With the sharpest notches, a detectable crack appeared very early in the fatigue life, showing that, in this case, the nucleation phase is almost negligible, thus providing another possible explanation for the observed reduction of the fatigue strength in this case compared with specimens with larger notch radii.

Modelling of all these aspects of the fatigue behaviour of the specimens used in this work is not trivial and certainly requires more investigation, particularly on the effect of self heating. However, numerical tools for including in finite element analyses part of the factors influencing the fatigue behaviour analysed in this work, namely the fibre orientation distribution obtained with different geometry and position of the injection gate, are already available. Therefore, the results presented herein could be used to validate numerical approaches based on finite element simulations conducted taking into account the dependence of the local mechanical properties on fibre orientation.

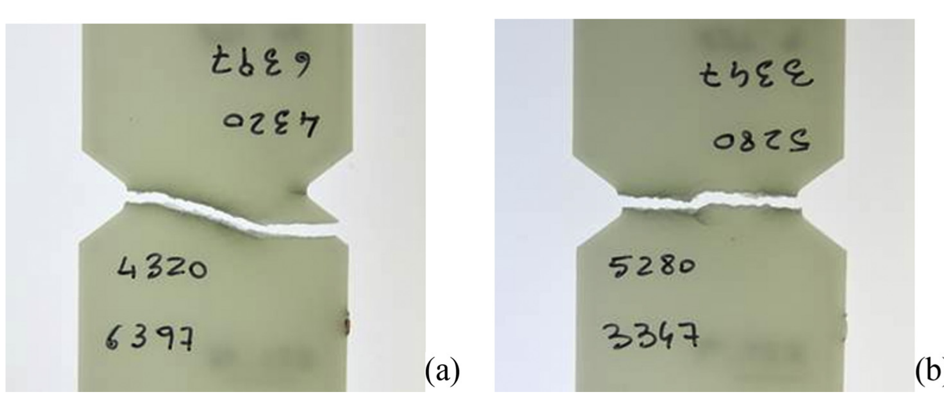

Fig. 11. Crack propagation paths at the end of fatigue tests: (a) side injection and (b) top injection.

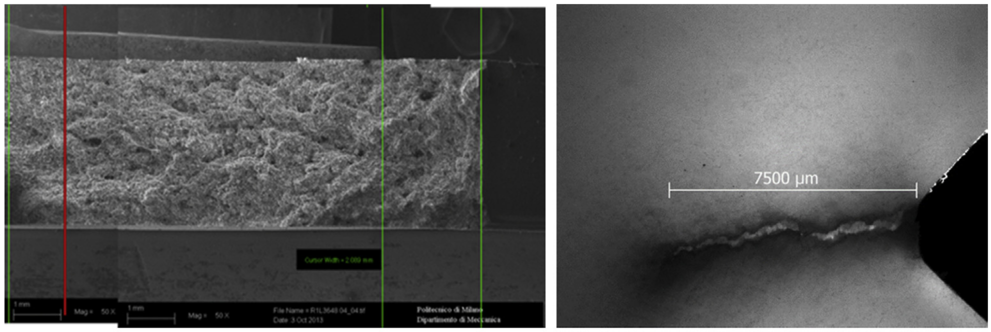

(a) (b)

Fig. 13. (a) position of the transition from micro-ductile to micro-brittle area (red line); (b) crack length measured before cryogenic fracture. (For interpretation of the references to colour in this figure legend, the reader is referred to the web version of this article.)

Acknowledgements

The specimens were provided by Radici Novacips SpA.

References

[1] J.F. Mandell, Fatigue behaviour of short fiber composite material, in: K.L. Reifsnider (Ed.), Fatigue of Composite Materials, Elsevier, Amsterdam, 1991.

[2] R.W. Hertzberg, J.A. Manson, Fatigue of Engineering Plastics, Academic Press, New York, 1980.

[3] N. Jia, V.A. Kagan, Effects of time and temperature on the tension-tension fatigue behavior of short fiber reinforced polyamides, Polym. Compos. 19 (4) (1998) 408–414.

[4] K. Handa, A. Kato, I. Narisawa, Fatigue characteristics of a glass-fiber-reinforced polyamide, J. Appl. Polym. Sci. 72 (13) (1999) 1783–1793.

[5] J.J. Horst, J.L. Spoormaker, Mechanism of fatigue in short glass fiber reinforced polyamide 6, Polym. Eng. Sci. 36 (22) (1996) 2718–2726.

[6] P.K. Mallick, Z. Yuanxin, Effect of mean stress on stress-controlled fatigue of a short E-glass fiber reinforced polyamide-6,6, Int. J. Fatigue 26 (9) (2004) 941–946.

[7] A. Bernasconi, R.M. Kulin, Effect of frequency upon fatigue strength of a short glass fiber reinforced polyamide 6: A superposition method based on cyclic creep parameters, Polym. Compos. 30 (2) (2009) 154–161.

[8] A. Bernasconi, P. Davoli, A. Basile, A. Filippi, Effect of fibre orientation on the fatigue behaviour of a short glass fibre reinforced polyamide-6, Int. J. Fatigue 29 (2) (2007) 199–208.

[9] M. De Monte, E. Moosbrugger, M. Quaresimin, Influence of temperature and thickness on the off-axis behaviour of short glass fibre reinforced polyamide 6.6 — cyclic loading, Compos Part A Appl. Sci. 41 (10) (2010) 1368–1379.

[10] B.R. Whiteside, P.D. Coates, P.J. Hine, R.A. Duckett, Glass fibre orientation within injection moulded automotive pedal. Simulation and experimental studies, Plast. Rubber Compos. 29 (1) (2000) 38–45.

[11] Y. Zhou, P.K. Mallick, Fatigue performance of an injection-molded short E-glass fiber-reinforced polyamide 6,6. I. Effects of orientation, holes, and weld line, Polym. Compos. 27 (2) (2006) 230–237.

[12] C.M. Sonsino, E. Moosbrugger, Fatigue design of highly loaded short-glass-fibre reinforced polyamide parts in engine compartments, Int. J. Fatigue 30 (7) (2008) 1279–1288.

[13] J. Hartmann, E. Moosbrugger, A. Büter, Variable amplitude loading with components made of short fiber reinforced polyamide 6.6, Proc. Eng. 10 (2011) 2009–2015.

[14] S. Castagnet, C. Nadot-Martin, A. Bernasconi, E. Lainé, E. Conrado, P. Caton-Rose, Through process modeling for the fatigue life assessment of notched injection-molded specimens, in: Proceedings of ECCM16-16th European Conference on Composite Materials, 22–26 June 2014. Seville, Spain.

[15] A. Bernasconi, F. Cosmi, E. Zappa, Combined effect of notches and fibre orientation on fatigue behaviour of short fibre reinforced polyamide, Strain 46 (5) (2010) 435–445.

[16] A. Bernasconi, F. Cosmi, P. Hine, Analysis of fibre orientation distribution in short fibre reinforced polymers: A comparison between optical and tomographic methods, Compos. Sci. Technol. 72 (16) (2012) 2002–2008.

[17] P.J. Hine, N. Davidson, R.A. Duckett, I.M. Ward, Measuring the fibre orientation and modelling the elastic properties of injection moulded long glass fibre reinforced nylon, Compos. Sci. Technol. 53 (2) (1995) 125–131.

[18] B. Klimkeit, Y. Nadot, S. Castagnet, C. Nadot-Martin, C. Dumas, S. Bergamo, C.M. Sonsino, A. Büter, Multiaxial fatigue life assessment for reinforced polymers, Int. J. Fatigue 33 (6) (2011) 766–780.

[19] P.J. Hine, R.A. Duckett, P. Caton-Rose, P.D. Coates, Fibre orientation structures and their effect on crack resistance of injection moulded transverse ribbed plate, Plast. Rubber Compos. 33 (1) (2004) 43–53.

[20] J.J. Horst, J.L. Spoormaker, Fatigue fracture mechanism and fractography of short-glassfibre-reinforced polyamide 6, J. Mater Sci. 32 (14) (1997) 3641–3651.

[21] V. Le Saux, Y. Marco, A. Launay, L. Jégou, S. Calloch, Infrared thermography: a powerful tool to characterize the thermomechanical and fatigue properties of short glass fiber reinforced thermoplastic structural samples, in: The Tenth International Conference on Multiaxial Fatigue & Fracture (ICMFF10), 2013. Kyoto (Japan).

[22] Y. Marco, V. Le Saux, L. Jégou, A. Launay, L. Serrano, I. Raoult, S. Calloch, Dissipation analysis in SFRP structural samples: Thermomechanical analysis and comparison to numerical simulation, Int. J. Fatigue 67 (2014) 142–150.